A R C H I V E S O F M E T A L L U R G Y A N D M A T E R I A L S
Volume 60 2015 Issue 3
DOI: 10.1515/amm-2015-0361

T. WIERZCHOŃ*#, E. CZARNOWSKA**, J. MORGIEL***, A. SOWIŃSKA**, M. TARNOWSKI*, A. ROGUSKA****

THE IMPORTANCE OF SURFACE TOPOGRAPHY FOR THE BIOLOGICAL PROPERTIES OF NITRIDED DIFFUSION LAYERS PRODUCED ON TI6AL4V TITANIUM ALLOY

ZNACZENIE TOPOGRAFII POWIERZCHNI DLA BIOLOGICZNYCH WŁAŚCIWOŚCI WARSTW AZOTOWANYCH DYFUZYJNIE WYTWARZANYCH NA STOPIE TYTANU TI6AL4V

Diffusion nitrided layers produced on titanium and its alloys are widely studied in terms of their application for cardiac and bone implants. The influence of the structure, the phase composition, topography and surface morphology on their biological properties is being investigated. The article presents the results of a study of the topography (nanotopography) of the surface of TiN+Ti_2N+αTi(N) nitrided layers produced in low-temperature plasma on Ti6Al4V titanium alloy and their influence on the adhesion of blood platelets and their aggregates. The TEM microstructure of the produced layers have been examined and it was demonstrated that the interaction between platelets and the surface of the titanium implants subjected to glow-discharge nitriding can be shaped via modification of the roughness parameters of the external layer of the TiN titanium nitride nanocrystalline zone.
Keywords: Ti6Al4V titanium alloy, glow discharge assisted nitriding, surface topography, wettability, blood platelets

Dyfuzyjne warstwy azotowane na tytanie i jego stopach są szeroko badane m. in. w aspekcie zastosowań na implanty kardiologiczne i kostne. Stąd też analizowany jest wpływ struktury składu fazowego, topografii i morfologii powierzchni na ich właściwości biologiczne. W artykule przedstawiono wyniki badań wpływu topografii (nanotopografii) powierzchni warstw azotowanych –TiN+Ti_2N+αTi(N) wytwarzanych w niskotemperaturowej plazmie na stopie tytanu Ti6Al4V na adhezję płytek krwi i ich aglomeratów. Omówiono mikrostrukturę (TEM) wytwarzanych warstw i wykazano, że poprzez stan chropowatości powierzchni zewnętrznej strefy warstwy azotowanej – nanokrystalicznego azotku tytanu (TiN) można kształtować oddziaływanie płytek krwi z powierzchnią implantów tytanowych poddanych procesowi azotowania jarzeniowego.

1. Introduction

The properties of titanium biomaterials are modified by means of surface engineering methods, which make it possible to produce surface layers with a controlled phase composition, microstructure, surface topography and residual stresses. These features affect such functional properties as hardness, wear resistance, mechanical properties, biological properties and wettability. In order to modify the properties of biomaterials, different methods of surface treatment are used, ranging from electrochemical oxidation, thermal spraying, ion implantation, laser treatment (PLD), chemical vapour deposition (RFCVD, MWCVD), to hybrid and glow-discharge methods [1-20]. Selection of the appropriate method depends on the final application of the material, the implant's shape and the expected characteristics of the produced surface layers. In light of the high level of chemical affinity between titanium and nitrogen, in particular of atomic nitrogen formed in low-temperature glow-discharge plasma [21], and by taking advantage of the phenomenon of cathodic sputtering in the shaping of the topography of the treated surfaces, one of the most promising methods of processing titanium and its alloys for medical applications is nitriding in low-temperature plasma. This process can be applied for titanium alloys at reduced temperatures starting from 300°C [22,23]. However, in the case of Ti6Al4V alloy, which is commonly used in medicine

* WARSAW UNIVERSITY OF TECHNOLOGY, WARSZAWA, POLAND
** CHILDREN'S MEMORIAL HEALTH INSTITUTE, WARSZAWA, POLAND
*** INSTITUTE OF METALLURGY AND MATERIALS, SCIENCE POLISH ACADEMY OF SCIENCES, 30-059 KRAKOW, POLAND
**** INSTITUTE OF PHYSICAL CHEMISTRY, POLISH ACADEMY OF SCIENCES, WARSZAWA, POLAND
# Corresponding author: twierz@inmat.pw.edu.pl

especially for bone implants, a minimum processing temperature of 680°C is required to maintain the required mechanical properties [2,24]. The surface layers formed are diffusive in nature and can be produced on complexly-shaped parts. They also possess titanium nitride (TiN) in the external zone, which is characterised by good biocompatibility and resistance to wear by friction [8,16,19,20]. Depending on the structure and surface topography of the layer, its biological properties, such as haemocompatibility, can be modified. This is of particular importance for cardiac implants, which include heart valve rings, stents or artificial pump impeller parts [25,26]. In spite of the extensive research of surface roughness on the biology of cells, no clear criteria that describe the characteristics of the topography of the surface of titanium nitride in terms of restricting blood clotting have been determined. The literature states that the nanotopography of the surface has a significant effect on biofilm composition and adhesion processes and on the differentiation of cells [8,23,27,28]. However, the biological processes listed are modified not only by the phase composition of the surface layer and surface topography, but also by the wettability of the surface [29,30].

The aim of the paper was to assess the impact of the surface topography of TiN+Ti_2N+αTi(N) surface layers with a nanocrystalline TiN external zone, produced on Ti6Al4V titanium alloy in low-temperature plasma [24], on their wettability, platelet adhesion and formation of aggregates.

2. Materials and Methods

The nitrided layers were produced on ϕ8×0,8 mm samples by means of glow-discharge nitriding process in the following conditions: process temperature – T = 680°C, process time – t = 4 h, pressure in the working chamber – p = 200 Pa in a so-called dynamic vacuum, i.e. at a constant flow rate (ca. 100 ml/min of a 99.99% nitrogen gas mixture containing 5% vol. of hydrogen) through the working chamber. Some of the samples, immediately before the nitriding process, were subjected to cathodic sputtering at 600°C for 30 mins, at a pressure of 30 Pa in an atmosphere of argon mixed with hydrogen – 5% vol. (samples designated as TiN-CS). The topography of the TiN+Ti_2N+αTi(N) nitride surface layers was influenced by mechanical processing, i.e. grinding using sandpaper with a grit size of up to 1000, and polishing in a diamond suspension with silicon oxide with a grain size of 0.04 μm (samples designated as – TiN). Some of the samples designated as TiN-G were ground only using 320 grit sandpaper. The surface layer microstructure was investigated using a TECNAJG^{2}FEG Super TWIN (200 kV) transmission electron microscope equipped with a High Angle Annular Dark Field (HAADF) detector and an EDAX Energy Dispersive Spectroscopy (EDS) system. The thin foils of the surface layer cross-section were cut using Focused Ion Beam (FIB) Quanta 3D with Omniprobe pick-up attachment. Afterwards, an approximately 50 nm thick carbon coating was deposited to separate the surface layer from the platinum used in this technique as a mask protecting the surface features and maintaining the image contrast. Phase analysis was performed using a Brucker D-8 Advance X-ray diffractometer with a CuK_α lamp. Surface topography was characterized by a Veeco atomic force microscope with a Multimode VIII controller (tapping mode, tip model ACSTA, AppNano). Wettability was determined in deionised water and ethylene glycol (goniometer OCA-15 DataPhysik).

The samples used for the biological tests were subjected to plasma sterilization (Sterrad 100, H_2O_2 atmosphere, 54°C, 7hPa), and after sterilization, to X-ray electron spectroscopy (XPS) in order to determine the chemical composition of the surface, which was carried out using a Microlab 350 (Thermo Electron Corporation) spectrometer with XPS. Excitation was performed using X-ray radiation with an energy of hv = 1486.6 eV (AlK_α). The pressure used in the measurement was $5 \cdot 10^{-7}$ Pa.

XPS spectra were registered at analyser transition energies of 150 and 40 eV (the maximum energy resolution for the device was 0.83 eV). The spectra recorded in the narrow bond energy range were deconvolved by the deconvolution procedure using the Gaussian/Lorentzian asymmetric function. The energies measured for the particular elements were corrected based on the bond energy of coal C1s = 285 eV (C-C bond).

Biological tests were then carried out of the influence of the surface topography on adhesion and blood platelet aggregation. For this purpose, platelet-free plasma and platelet-rich plasma (PRP) taken from healthy blood donors was incubated for 2h at T = 37°C on nitrided samples with varying degrees of coarseness. The adhered blood platelets, which were preserved using a 4% buffered glutaraldehyde, then dehydrated, dried and sputtered with a ca. 10 nm layer of gold (using a JFC-1200 Jeol Fine Coater) were studied under a scanning electron microscope (Jeol JSM 7600F). Morphometric analyses of the blood platelets were carried out using CellSense (Olympus) morphometric software.

3. Results and discussion

The TiN+Ti_2N+αTi(N) nitrided layers produced were diffusive. The nitrided layer produced in the low-temperature process was ca. 4 μm thick. The microstructure (TEM) and distribution of the Ti, N, Al, V elements, as well as electron diffraction and x-ray diffraction patterns are shown in (Fig. 1).

The examination revealed a zonal structure of the nitrided surface layers produced in the low temperature plasma nitriding process. The upper zone was built of nano-crystallites of TiN, directly below there was a fine-crystalline zone of Ti_2N, and the third zone consisted of irregular crystallites of αTi(N) and $TiAl_3$ phase precipitates, which was demonstrated by earlier tests [24]. Titanium nitride – the TiN outer zone, was about 1 μm thick and was characterized by a high density. X-ray diffraction of the studied layers revealed the presence of TiN and Ti_2N nitrides. As a result of nitriding, the lattice parameters of αTi phase in nitrided layer were changed. For the initial state they were: a,b = 0.292 nm, c = 0.468 nm, whereas after nitriding they amounted to: a,b = 0.295 nm, c = 0.473 nm respectively. Nitrogen

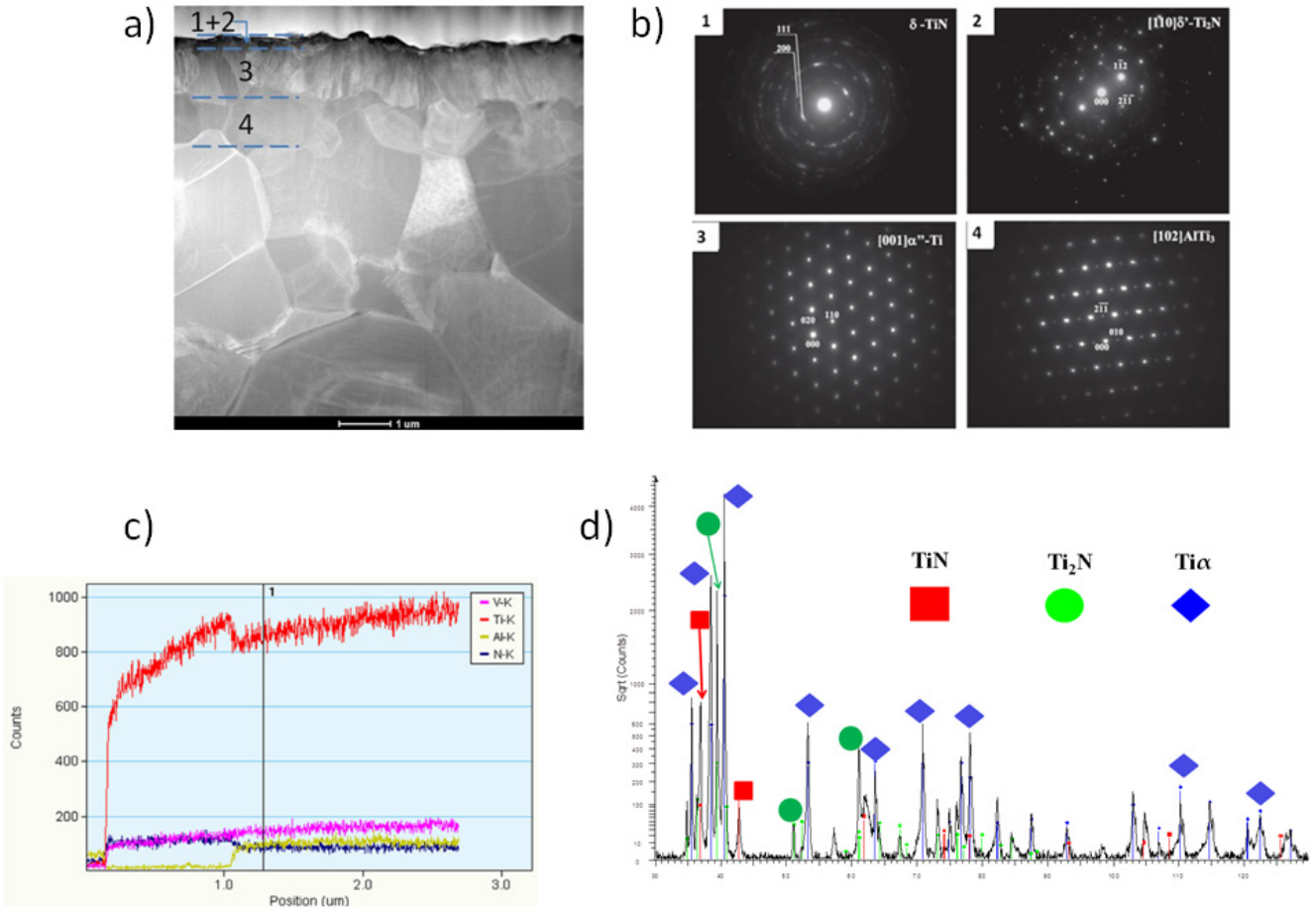

Fig. 1. TEM BF image of the near-surface zone of nitrided layer produced on Ti6Al4V alloy at 680°C (a), electron diffraction patterns from 1-4 sublayers (b), elements' distribution in the cross-section (c), and x-ray diffractogram of the surface layer (d)

diffusion to phase αTi caused lattice expansion, which is depicted by a shifting of the peaks of this phase (Fig. 1d).

(Fig. 2) presents an XPS spectrum of the surface of the nitrided Ti6Al4V titanium alloy before and after plasma sterilisation.

The XPS spectrum revealed titanium, nitrogen and adventitious carbon in the nitrided layer both before and after sterilisation. The chemical composition analysis results of the examined surfaces are presented in (Table 1).

TABLE 1

XPS chemical composition analysis for the TiN+Ti_2N+αTi(N) layer before and after plasma sterilisation

Material	Concentration [at. %]			
	C	Ti	O	N
TiN+Ti_2N+αTi(N) before plasma sterilisation	14,3	33,3	9,9	37,9
TiN+Ti_2N+αTi(N) after plasma sterilisation	7,4	39,8	12,0	40,8

(Table 2) presents the bond energy and the chemical state of the elements present on the surface of the nitrided Ti6Al4V titanium alloy after glow-discharge nitriding and plasma sterilisation.

An analysis of the bond energy revealed the presence of TiN titanium nitrides, TiO_xN_y oxynitrides and TiO_2 titanium oxides on the examined nitrided surface layers after sterilisation. This proves that partial oxidation takes place on the surface layer of TiN as a result of plasma sterilisation. It is known as a fact that titanium oxynitrides and titanium oxide (TiO_2) demonstrate good biological properties [11,20]. The phase composition of the surface has been shown to be the same for all the tested nitrided layers, which allow us to conclude that the micro- and nano-roughness of the TiN surface, i.e. the external zone of the nitrided layer, has a decisive impact on the adhesion of blood platelets and their aggregates.

It should be noted that as a result of glow discharge nitriding conducted by cathodic sputtering, the outer zone of the nitrided surface layer – TiN, had a strongly developed surface in the nanoscale (Fig. 3, Table 3), which can be additionally modified by grinding the Ti6Al4V titanium alloy before the nitriding process (Table 3 – TiN-G).

The surfaces of the studied samples differed significantly in terms of topography and surface wettability (Table 3, 4). Nitrided layers formed on the Ti6Al4V titanium alloy were shown to have the highest degree of roughness (TiN-G), whereas the

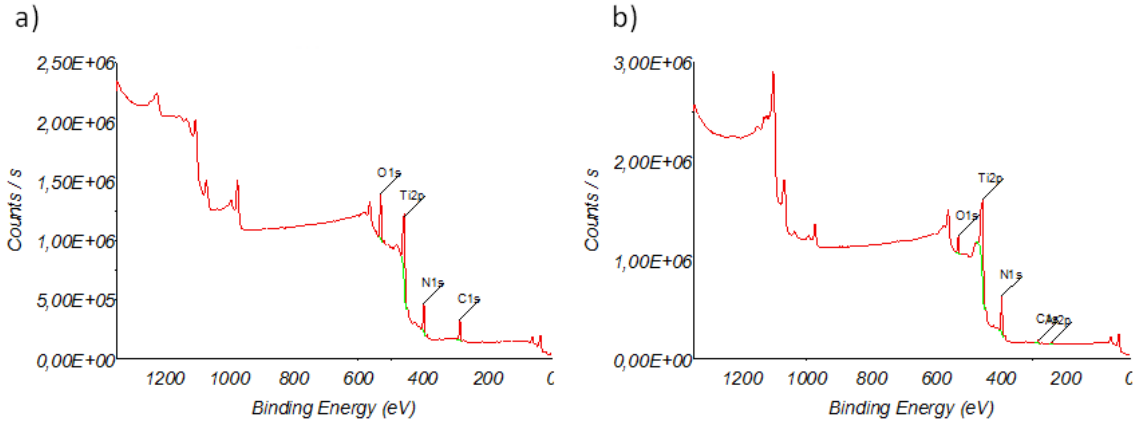

Fig. 2. XPS spectrum of the titanium nitride – TiN surface on the nitrided Ti6Al4V titanium alloy before and after plasma sterilisation

TABLE 2

Bond energy and the chemical state of elements present on the surface of the nitrided Ti6Al4V titanium alloy before and after plasma sterilisation

	TiN+Ti_2N+αTi(N) before plasma sterilisation			**TiN+Ti_2N+αTi(N) after plasma sterilisation**		
Line	**Bonding energy [eV]**	**Chemical state**	**Atomic %**	**Bonding energy [eV]**	**Chemical state**	**Atomic %**
C1s	285,0	C-C, C-H	51,2	285,0	C-C, C-H	23,9
C1s A	287,2	C-O, C-OH	6,9	286,6	C-O, C-OH	4,6
C1s B	289,2	COOH	3,3	288,6	COOH	2,3
O1s	532,6	C=O, hydroxides (-OH) or TiO_xN_y	8,4	530,2	metal oxides	14,4
O1s A	530,5	metal oxides	7,0	531,9	C=O, hydroxides (-OH) or TiO_xN_y	5,7
O1s B	534,1	TiO_xN_y, H_2O	2,2	533,6	TiO_xN_y, H_2O	1,7
N1s	397,1	TiN	6,7	397,1	TiN	17,0
N1s A	399,8	TiO_xN_y	0,9	399,1	TiO_xN_y	2,1
N1s B	393,3	TiO_xN_y	3,8	396,0	TiO_xN_y	3,7
Ti2p3	455,5	TiN	3,6	458,4	TiO_2	12,6
Ti2p3 A	458,7	TiO_2	2,9	455,3	TiN	7,9
Ti2p3 B	457,1	TiO_xN_y	3,1			

highest wetting angle, both in deionised water and in ethylene glycol, was characteristic of TiN-CS layers, i.e. ones that additionally underwent cathodic sputtering (TABLE 4) and which demonstrated a greater degree of surface roughness in the nanometric scale (Fig. 3).

TABLE 3

Roughness of the studied nitrided layers (AFM)

Material	***Ra***	***Rq***	***Rt***
	[µm]		
Ti6Al4V after polishing	0,020	0,026	0,514
TiN+Ti_2N+αTi(N) surface layer (TiN)	0,025	0,038	0,913
TiN+Ti_2N+αTi(N) surface layer (TiN-CS)	0,177	0,229	3,244
TiN+Ti_2N+αTi(N) surface layer (TiN-G)	0,600	0,748	6,172

Abrreviation: *Ra* – average arithmetic deviation of the roughness profile, *Rq* – average square deviation of the roughness profile *Rt* – average differences between the 5 highest and the 5 deepest valleys in the roughness profile (acc. to ISO 4287/1-1984)

TABLE 4

Wetting angle of the materials' surface examined in the present experiments

Material	**Wettability [°]**	
	Deionized water	**Ethylene glycol**
Ti6Al4V after polishing	73,06±0,67	47,42±0,54
TiN+Ti_2N+αTi(N) surface layer (TiN)	72,80±0,45	47,75±0,59
TiN+Ti_2N+αTi(N) surface layer (TiN-CS)	74,06±0,61	55,24±0,71
TiN+Ti_2N+αTi(N) surface layer (TiN-G)	73,03±0,94	52,64±0,71

The wetting angle of surfaces with low *Ra* parameters (Ti6Al4V titanium alloy) in initial state (after polishing), that is surfaces with a spontaneously forming layer of TiO_2, TiO, Ti_2O_3 titanium oxides, characterised by an overall formless structure [31], and the contact angle of the nitrided layer formed on polished Ti6Al4V titanium alloy (TiN), were of the same order in the case of ethylene glycol, and increased along with the degree of surface roughness of TiN-CS and TiN-G nitrided layers.

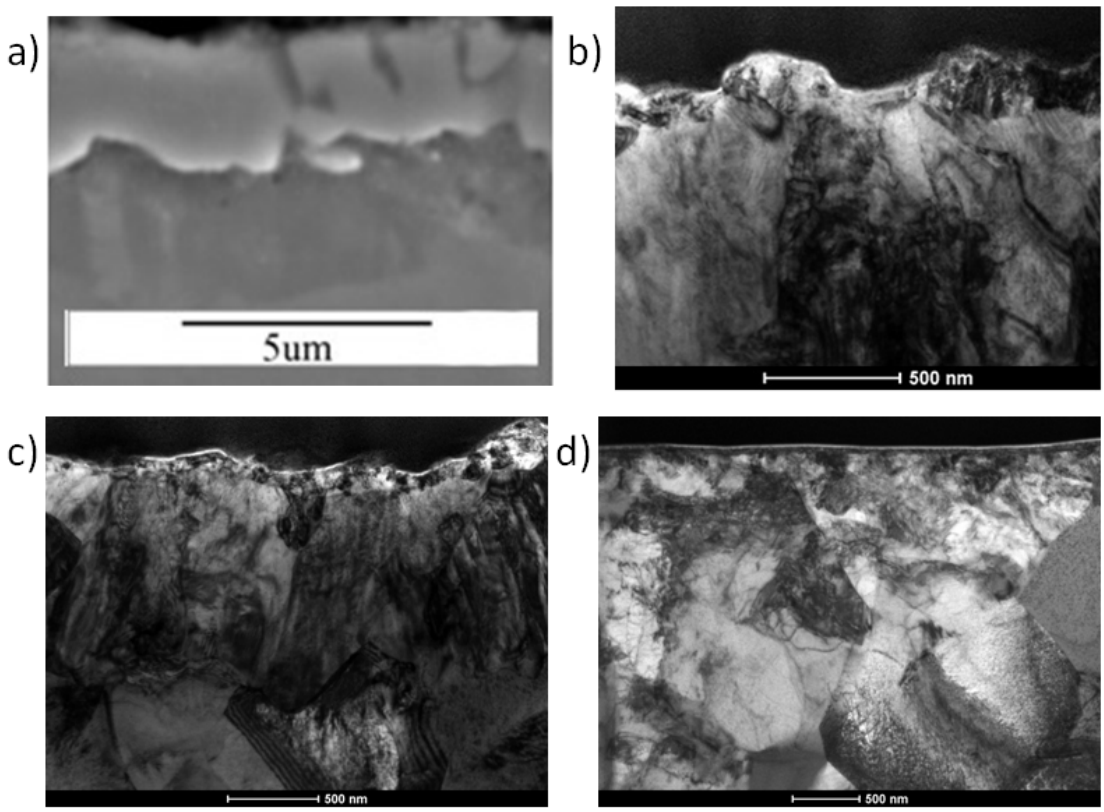

Fig. 3. SEM microstructure of nitrided layer (a) and TEM BF image of the TiN surface zone - TiN(CS) (b) and TiN(G) (c) compared to the nitrided layer formed on the polished titanium alloy (d)

The literature suggests that the increase in surface topography, especially in the nanometric scale, increases the ability of the surface to absorb protein, which influences both adhesion and activation of the blood platelets, as well as the proliferation of osteoblasts [27-29, 32]. Interestingly, experiments with PRP revealed lower platelet adhesion and aggregation on nitrided surface layers designated as TiN-CS with an intermediate roughness of $Ra = 0.177$ µm. The consecutive increase in surface roughness observed for TiN-G ($Ra = 0.600$) contributed both to an increase of platelet adhesion and to their activation (Fig. 4). Platelet activation was expressed by a change of their shape and size (Fig. 5).

This may result from the fact that the increase in surface roughness, especially in the nanometric scale, may contribute to conformance changes in the structure of the proteins forming the biofilm, which in turn affects blood platelet adhesion [8,33]. Our previous studies on oxynitrided layers [23] showed that more albumin, responsible for blocking platelet adhesion, is absorbed on the surface of TiO_2 with higher surface roughness.

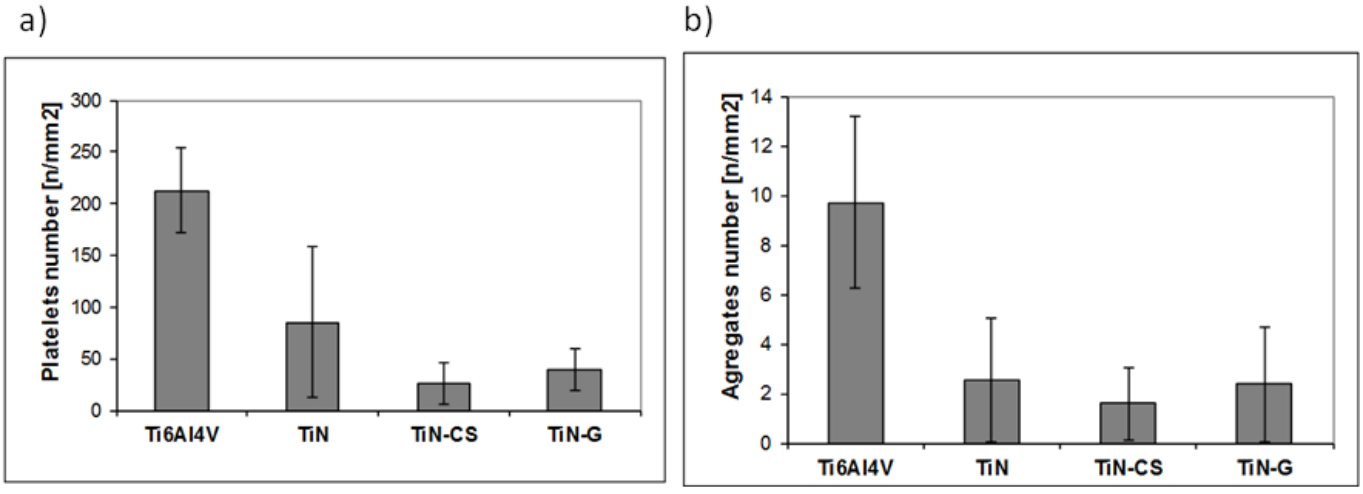

Fig. 4. Number of blood platelets (a) and platelet aggregates (b) on the tested materials

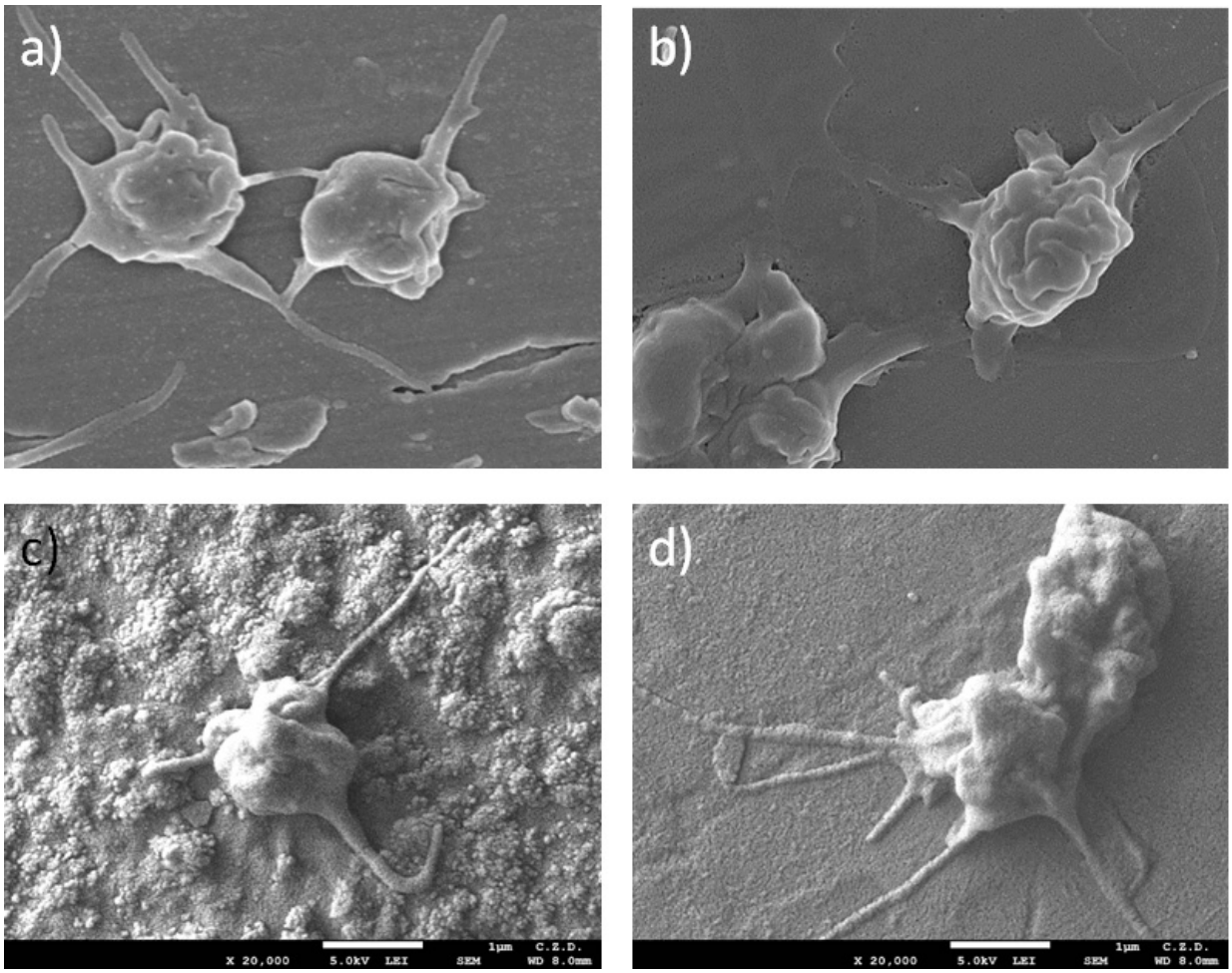

Fig. 5. Morphology of blood platelets adhering to polished Ti6Al4V titanium alloy (a) TiN+Ti_2N+αTi(N) layers formed on Ti6Al4V titanium alloy of varying degrees of roughness – *Ra* = 25 nm (b), TiN(CS); *Ra* = 177 nm (c) and TiN(G) – *Ra* = 600 nm (d)

Blood platelets which adhere to the TiN-CS layer were characterised by a dendritic shape with single protrusions, while in the case of surfaces displaying a lower (TiN) and higher (TiN-G) degree of roughness, the cells formed numerous protrusions, which was indicative of their greater activation. The biological effect of contact between the surface and the blood platelets also correlates with changes in the wettability of the surface (TABLE 4). A similar dependency between TiN layer roughness produced by direct current reactive magnetron sputtering and a decrease in adhesion and platelet activation was observed in the study [8].

4. Conclusion

The results of the study revealed that blood platelet adhesion and the formation of agglomerates depends on the roughness of the surface, especially the nanotopography of the nanocrystalline TiN layer - i.e. the TiN+Ti_2N+αTi(N) external zone of the nitrided layer. This is in close correlation with the contact angle parameters, which were shown to have the highest value in the case of the nitrided layer with a developed titanium nitride surface topography shaped by cathodic sputtering. Thus, by modifying the glow-discharge nitriding process, blood platelet adhesion and aggregation can be significantly reduced, which can be of great practical importance for the production of specific-purpose implants. This feature, in addition to the fact that nitrided layers on titanium and its alloys eliminate the metallosis effect and demonstrate a high resistance to wear by friction, as proven in previous studies [20], attests to the significant potential of this technology.

Acknowledgement

The study was financed by the National Science Centre as part of research projects 2011/01/D/ST8/02931 and 2011/01/B/ST8/07554.

REFERENCES

[1] K.S. Bramer, S. Odi, C.J. Cobb, L.M. Bjursten, H. van der Heyde, S. Jin, Acta Biomat. **5,** 3215 (2009).

[2] E. Czarnowska, J. Morgiel, M. Ossowski, R. Major, A. Sowińska, T. Wierzchoń, J. Nanosci. Nanotechno. **11,** 8917 (2011).

[3] M. Järn, S. Areva, V. Pore, J. Peltonen, M. Linden, Langmuir **22**, 8206 (2006).
[4] J. Zhao, X. Wang, R. Chen, L. Li, Solid State Commun. **134**, 705 (2005).
[5] S.J. Shabalovskaya, S.J. Anderegg, J. Van Humbeeck, Acta Biomat. **4**, 447 (2008).
[6] X. Lin, P.K. Chu, C.X. Ding, Mat. Sci. Eng. R. **47**, 49 (2004).
[7] A. Zhecheva, W. Sha, W. Malinov, S. Long, Surf. Coat. Tech. **200**, 2192 (2005).
[8] V. Karagkiozaki, S. Logothetidis, N. Kalfagiannis, S. Lousinian, G. Giannoglou, Nanomed.-Nanotechnol. **5**, 64 (2009).
[9] M. Gołębiewski, G. Krużel, R. Major, W. Mróz, T. Wierzchoń, R. Ebner, B. Major, Mater. Chem. Phys. **81**, 315 (2002).
[10] K. Bordji, J.Y. Jouzeau, D. Mainard, E. Payan, P. Netter, K.T. Rie, T. Stucky, M. Hage-Ali, Biomaterials **17, 9**, 929 (1995).
[11] M. Bakir, J. Biomater. Appl. **27**, 3 (2012)
[12] M.I. Jones, J.R. McColl, D.M. Grant, K.G. Parker, T.L. Parker, J. Biomed. Mater. Res. **52**, 413 (2000).
[13] B. Major, W. Mróz, T. Wierzchoń, W. Waldhauser, J. Lackner, R. Ebner, Surf. Coat. Tech. **180-181**, 580 (2004).
[14] M.C. Sunny, C.P. Sharma, Surf. Coat. Tech. **174-175**, 591 (2003).
[15] N. Huang, Y.R. Chen, X.H. Liu, J. Biomater. Appl. **8,** 404 (1994).
[16] A. Geetha, A.K. Sing, R. Asokamani, A.K. Gogia, Prog. Mater. Sci. **54**, 397 (2009).
[17] M. Raaif, F.M. El-Hossany, N.Z. Negm, S.M. Khalil, D. Shaaf, J. Phys. Condens. Mater. **19**, 396003 (2007).
[18] D.B. Lee, M.J. Kim, L. Chen, S.H. Bak, O. Yasikov, V. Fedirko, Met. Mater. Int. **17**, 471 (2011).
[19] C. Alves Jr, C.L. B. Guerra Netto, G.H.S. Moraias, C.F. da Silva, V. Hajek, Surf. Coat. Tech. **194**, 196 (2005).
[20] E. Czarnowska, T. Wierzchoń, A Maranda-Niedbała, E. Karczmarewicz, J. Mat. Sci.-Mater. M. **11**, 73 (2000).
[21] T. Burakowski, T. Wierzchoń, Surface Engineering of Metals: principles, technologies, applications, CRC Press, Boca Raton, New York 1999.
[22] R.R.M. de Sousa, F.O. de Araújo, K.J.B. Ribeiro, M.W.D. Mendes, J.A.P. de Costa, C. Alves Jr, Mater. Sci. and Eng. A **465**, 223 (2007).
[23] E. Wierzchoń, E. Czarnowska, J. Grzonka, A. Sowińska, M. Tarnowski, J. Kamiński, K. Kulikowski, T. Borowski, K. Kurzydłowski, Appl. Surf. Sci. **334**, 74 (2015).
[24] J. Morgiel, T. Wierzchoń, Surf. Coat. Tech. **259**, 473 (2014).
[25] Z. Nawrot, Adv. Biomed. Eng. **1**, 1 (2009).
[26] D. Brunette, P. Tengvall, M. Textor, P. Thomsen, Titanium in medicine, Springer-Verlag, Berlin, Heidelberg, 2001.
[27] D. Khang, J. Lu, C. Yao, K.M. Haberstroch, T.J. Webster, Biomaterials **29**, 970 (2008).
[28] Vandrovcova, J. Hamus, M. Drabik, O. Kylian, V. Lisa, L. Bacakova, , J. Biomed. Mater. Res. A **100**, 1016 (2012).
[29] T. Sawase, R. Jimbo, K. Baba, Y Shibata, T. Ikeda, M. Atsuta, Clin. Oral Implan. Res. **19**, 491 (2008).
[30] R. Kriparamanan, P. Aswath, A. Zhou, L. Tang, K.T. Nguyen, J. Nanosci. Nanotechnol. **6**, 1905 (2006).
[32] A. Sowińska, M. Tarnowski, W. Jakubowski, J. Oleksiak. T. Wierzchoń, E. Czarnowska, Eng. Biomater. **119**, 27 (2013).
[33] B. C. Cook, Tromb. Reasearch **104**, 39 (2001).
[34] A. Dolatshuhi-Pirouz, S. Skeldal, M.B. Hovgaard et. al., J. Phys. Chem. **113**, 4406 (2009).

Received: 20 April 2015.